Geophys. J. Int. (2003) **153,** 187–200

Possible mechanisms of magma redistribution under Mt Etna during the 1994–1999 period detected through microgravity measurements

D. Carbone, G. Budetta and F. Greco

Istituto Nazionale di Geofisica e Vulcanologia, Sezione di Catania, Piazza Roma 2, 95123 *Catania, Italy. E-mail: carbone@ct.ingv.it*

Accepted 2002 October 23. Received 2002 October 8; in original form 2002 April 3

SUMMARY

We analyse a microgravity data set acquired along the Etna network and spanning a 5 year long period (1994–1999). The main feature observed is a complete gravity increase (1994–1996)–decrease (1997–1999) cycle mainly affecting the southeastern sector of the volcano and reaching a maximum amplitude of approximately 100 μGal peak-to-peak. The gravity changes are principally due not to elevation changes but rather to the direct gravitational effect of magma accumulation and drainage below the volcanic pile. In particular, a complete mass increase–decrease cycle took place within a 2–4 km bsl deep reservoir that is elongated, oriented NNW–SSE, and lies in the southeastern sector of the volcano. The observed cycle accounts for a volume of magma ranging between 3 and 10×10^8 m^3, which is believed to have passed through the inferred reservoir between 1994 and 1999. Since most of this magma has not been erupted nor accumulated at shallower levels (at the summit Etna stations a compatible gravity increase has not been observed), it could have been recycled by the Etna plumbing system, sinking down to a level deeper than that of the inferred source.

Key words: array, density, gravity, magma, reservoirs, volcanic activity.

1 INTRODUCTION

The study of microgravity changes has been shown to provide precious pieces of information concerning the subsurface mass redistributions occurring in active areas. In particular, movements and/or density changes of subsurface magma bodies have been detected at many active volcanoes around the world and associated with the ongoing volcanic activity (Jachens & Eaton 1980; Sanderson 1982; Eggers 1983; Rymer & Brown 1987; Berrino *et al.* 1992; Rymer *et al.* 1993, 1995, 2000; Budetta & Carbone 1998; Budetta *et al.* 1999).

It is approximately 15 years since microgravity observations were started at Mt Etna (Budetta *et al.* 1989). These observations have allowed mass redistributions occurring at depths ranging between approximately 6 km bsl and a few hundred metres below the surface (magma level changes within the shallower parts of the feeding conduits) to be detected. In particular, a gravity increase for 2 years before the 1989 eruption was detected and was attributed to accumulation of magma in an elongate zone oriented NNW–SSE, between 2.5 and 6 km below sea level (Budetta & Carbone 1998). The subsequent sudden gravity decrease was attributed to magma drainage from this source zone. This magma supplied the 1989 and 1990 eruptions and also probably fed the start of the 1991–1993 eruption, since this event was not preceded by significant mass changes at the inferred source zone (Budetta & Carbone 1998). A large gravity increase, detected across the volcano between 1992 June and September, is consistent with the arrival in the same accumulation zone of new magma, thus favouring continued flank effusion until 1993 (Budetta & Carbone 1998). A decrease in magma level in the conduits feeding the summit craters of Etna during the closing stages of the 1991–1993 event could also be detected through analysis of gravity variations by Budetta & Carbone (1998).

Gravity changes detected at Mt Etna between 1994 and 1999 are presented and discussed in the following. Data acquired during the 1994–1996 period were already analysed by Budetta *et al.* (1999) and just some of them are presented again in the next sections to both provide a more complete picture of the changes observed at Mt Etna after the 1991–1993 eruption and to improve some of the previous estimates (such as the gravity effect of the water-table fluctuations at Mt Etna) on the grounds of the new data now available.

2 MICROGRAVITY MEASUREMENTS AT MT ETNA

2.1 The Etna gravity network

Gravity measurements have been carried out at Mt Etna since 1986. The gravity network (Fig. 1) is now composed of 69 stations 0.5–3 km apart, covers an area of approximately 400 km^2 and consists of four integrated subarrays (Budetta & Carbone 1998; Budetta *et al.* 1999):

(1) the main network (established in 1986) of 27 stations, separated by distances of 3–4 km, are arranged as a ring around the volcano at elevations of between 800 and 2000 m asl;

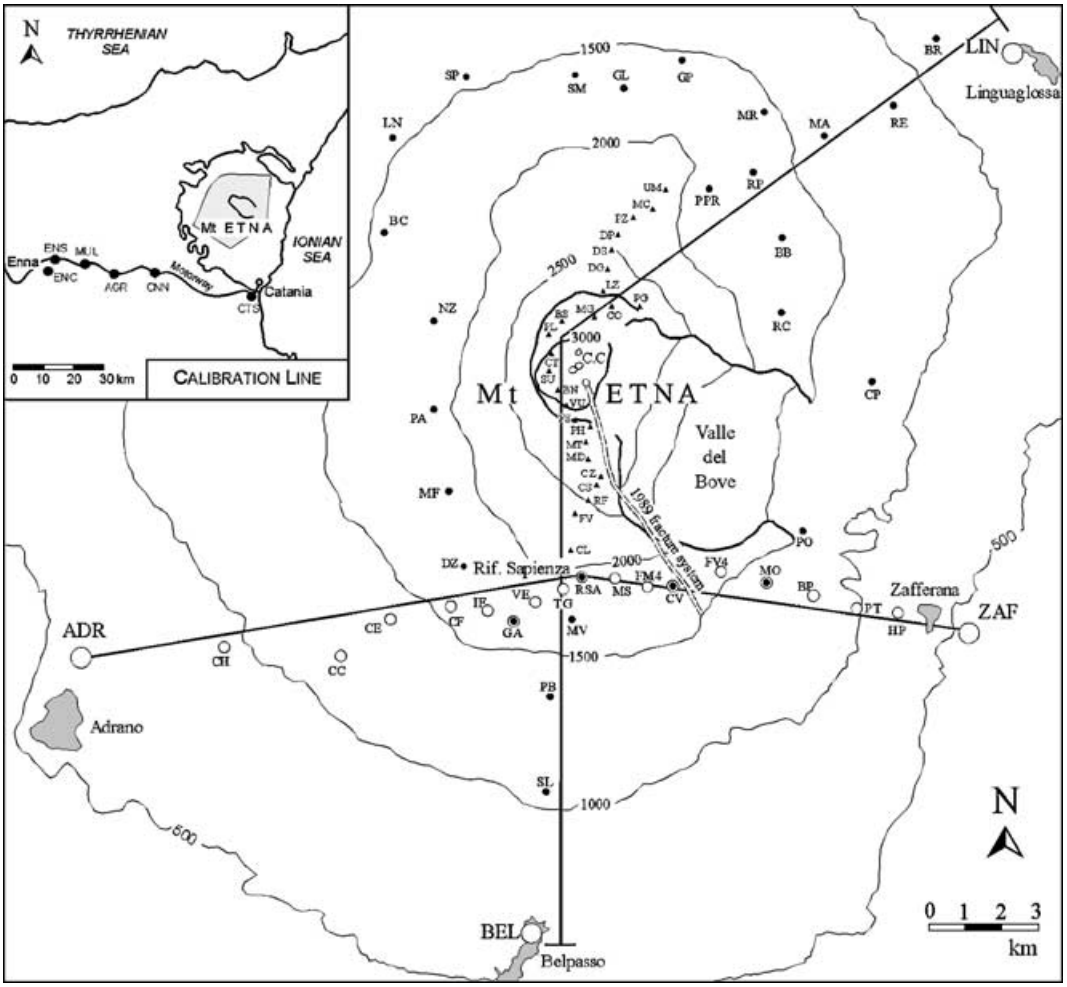

Figure 1. Sketch map of Mt Etna showing: (a) stations on the main network (filled circles), (b) the summit profile (triangles), (c) the east–west profile (small open circles) and (d) the Basal Reference Network (large open circles). The traces of the E–W and summit profiles (lines) and stations on the calibration line (filled circles, inset) are also shown. The shaded area in the inset represents the area covered by the gravity network.

(2) the summit profile (established in 1992) of 27 stations (two in common with the main network), arranged along a N–S line from Piano Provenzana (at the lowest elevation of 1770 m asl) to the Rifugio Sapienza crossing the summit zone; all stations are sited within 1 km of each other;

(3) the east–west profile (established in 1994) of 19 stations (four in common with the main network,) between Zafferana (450 m asl) and Adrano (600 m asl), connecting with the summit array at the Rifugio Sapienza and

(4) a base reference network (established in 1994) of four stations (two in common with the E–W profile) placed at the towns of Adrano, Belpasso, Zafferana and Linguaglossa, each of which is considered to be stable with respect to volcanic activity; all the other networks are connected to this reference network.

A calibration line was also established in 1995 February to investigate systematic variations in instrumental calibration factor with time. The line runs 80 km along the motorway from Catania to Enna and consists of six stations (Budetta & Carbone 1997; Carbone 2001, Fig. 1). The total gravity range along the line is 365 mGal (1 mGal $= 10^4$ nm s^{-2}), a result of (1) the height difference (940 m between CTS and ENC), and (2) a large negative gravity anomaly of approximately -150 mGal (AGIP 1976) across the line, linked to low-density sediments (approximately 10 km thick). About one-half of the range covered by the line overlaps the high edge of the 600 mGal range of Etna. Carbone & Rymer (1999) have demonstrated that, at least for L&R meters, calibration changes have the same percentage extent across the measuring range within experimental error. Any local instabilities (unlikely to exceed $\sim$cm yr^{-1}) or seasonal effects (e.g. owing to changes in the level of the water table) along the calibration line are expected to be approximately 10 μGal or less (1 μGal $= 10$ nm s^{-2}); such local errors can be identified and removed by a comparison of gravity changes on the six stations across the calibration line.

2.2 Gravity measurements along the Etna network

The subarrays have different characteristics regarding the density of the traverse, access to stations (determined by snow coverage) and the time required to make measurements. Each subarray can be occupied independently, optimizing the flexibility in making measurements to accommodate the changeable activity and accessibility of the volcano and, since each subarray is connected to the base reference network, data are always comparable with each other. Measurements are made with an automated, digital Scintrex

CG-3M gravimeter (serial number 9310234; Budetta & Carbone 1997). Measurements over the whole array are usually conducted every 6 months by the step method (Watermann 1957), in which adjacent stations are connected at least three times. Some parts of the array are reoccupied more frequently (approximately monthly measurements along the E–W and summit profiles, although snow coverage restricts measurements along the summit profile to the June–October period). Because of the more frequent measurements and the high station density (at least 1 station km^{-1}), the E–W and summit profiles provide the core microgravity data for Etna. Stations along the calibration line and summit profile are occupied in sequence, the arrays being traversed at least two (summit profile) or three (calibration line) times for each survey (profile method; Watermann 1957).

2.2.1 Control of instrumental drift and the calibration factor

The regular control of instrumental drift and the calibration factor are fundamental to maintaining high precision with the Scintrex CG-3M gravimeter. The stationary component of the drift of CG-3M is very strong but is almost linear over intervals of a few days. Drift can therefore be accurately forecast and the effect removed by the automatic real-time compensator of the instrument, to standards suitable for our purposes (a few tens of μGal d^{-1}; Budetta & Carbone 1997; Carbone 2001).

The first measurements made at Etna with Scintrex CG-3M 9310234 between 1994 and 1995 strongly suggested that the meter could have been affected by a gradual increase in the instrumental calibration factor since large (apparent) gravity changes were observed during a quiescent period and a strong correlation between gravity change and gravity value was detected at every station. Accordingly, a new calibration line was established in 1995 February to investigate systematic variations in the calibration factor (f) with time (Fig. 1). A significant positive correlation was found between gravity changes with time and gravity values along the line (regression coefficients >0.9, standard errors of estimate between 2.3 and 6.1 μGal (6–16 ppm)). Data from the calibration line have been combined with data previously assessed along the E–W profile to describe the changes in f since the first campaign of CG-3M 9310234 at Etna (Budetta & Carbone 1997). A gradual calibration factor increase of approximately 1250 ppm was determined between 1994 August, when the instrument was first used, and 1995 August (Budetta & Carbone 1997; Carbone 2001, Fig. 2). After a lower-rate decrease during the next year (approximately 250 ppm between 1995 August and 1996 August), the calibration of the instrument stabilized (Fig. 2) with a standard deviation of just 37 ppm (corresponding to 13.5 μGal over the 365 mGal range of the calibration line), very close to the uncertainty on each f-estimate along the line (typically 32 ppm at the 95 per cent confidence interval). In 1997 August CG-3M 9310234 was sent to Canada for servicing. Its calibration abruptly changed afterwards (Fig. 2), but the subsequent calibration shifts were close to the values for the previous year (standard deviation over the 1998 February–1999 June period (seven points) of 50 ppm). The importance of properly correcting for uncertainties in instrument calibration are to be stressed. Even the small error of 32 ppm on each f-estimate along the line could generate a fictitious gravity change of ±10 μGal along the E–W profile of Etna (gravity range of 300 mGal) and ±20 μGal over the complete microgravity network of Etna (gravity range of 600 mGal). Correlation studies provide a simple and efficient method of estimating changes in f with time and, thereby, of identifying and eliminating any such fictitious anomalies.

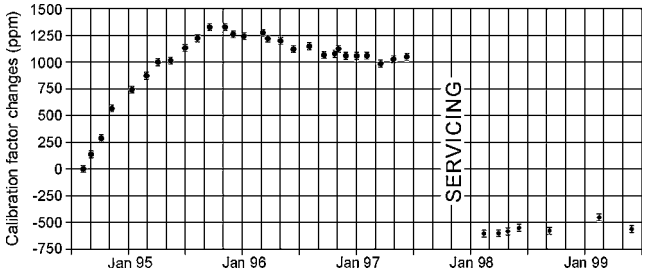

Figure 2. Time variation of the CG-3M calibration factor, derived from field data along the calibration line of Etna. The variations are referred to 1994 August measurements, in which the value of f supplied by the manufacturer was assumed.

2.2.2 Precision of measurements performed on Etna with the Scintrex CG-3M gravimeter

To evaluate the precision of the Scintrex CG-3M 9310234 gravimeter under the conditions encountered on Mt Etna, the instrument was site tested during the first year of its employment (Budetta & Carbone 1997). Using 471 gravity differences (Δg) obtained between 18 pairs of stations along the E–W profile (asphalted roads, stations less than 2 km apart), a standard deviation of the differences of Δg from the average values of each campaign of 3.5 μGal was calculated (Budetta & Carbone 1997, Fig. 3). We came to the same result using 69 Δg values obtained between 12 pairs of stations (3–6 km apart) on dirt tracks (main network). In the case of 28 Δg values gathered between five pairs of stations belonging to the base reference network (stations 20–50 km apart), the standard deviation of the differences of the Δg values from the average values of each campaign was 4.4 μGal (Budetta & Carbone 1997). The above standard deviations imply uncertainties of ±7 μGal (affecting measurements along the E–W profile and main network) and ±9 μGal (affecting measurements along the base reference network), respectively, at the 95 per cent confidence interval. The profile method (Watermann 1957, Section 2.2), which is normally used to survey the summit profile because of logistic reasons (difficulty in manoeuvring a car along the narrow and dirty road crossing the summit Etna zone, the necessity of

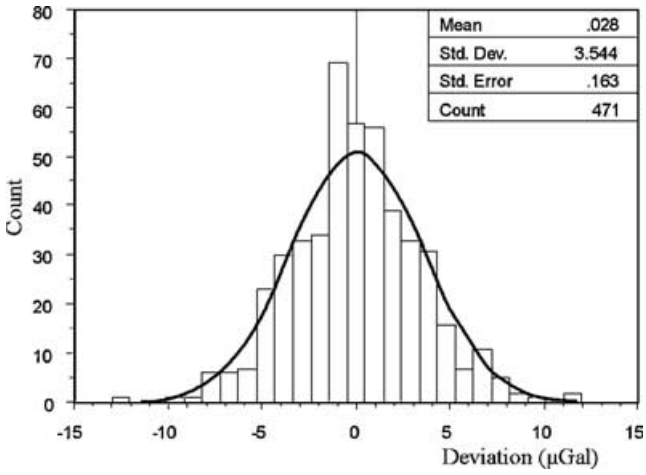

Figure 3. The standard deviation of the differences of Δg from the average values for each measuring campaign. The 471 measurements were obtained with the CG-3M during nine separate campaigns along the E–W profile of Etna between 1994 and 1995. Measurements were made between 18 pairs of stations connected by asphalted roads (from Budetta & Carbone 1997).

accomplishing the measurements as fast as possible to minimize the exposure of personnel during paroxysmal activity, etc.), implies errors larger than those affecting subarrays with stations separated by the same distance (E–W profile and main network) which are measured using the step method. These larger errors are caused by transport drift (Torge 1989), which is the effect of mechanical and thermal shocks, feature a marked non-linear behaviour and become more important when the profile method is followed because the gravimeter is driven for a longer time before a given station is re-occupied. The standard deviation of 237 differences between measurements obtained at each station of the summit profile during a single campaign is 5.8 μGal, yielding an uncertainty of ±11 μGal at the 95 per cent confidence interval. The error in temporal gravity differences is estimated by calculating $\sqrt{2} \times e$ (Rymer 1989), where e is the error on a single survey. Thus, at the 95 per cent confidence interval, the error on temporal gravity differences along the E–W profile is 10 μGal, while the error on temporal gravity differences along the summit profile is 15 μGal.

3 VOLCANIC ACTIVITY DURING THE 1997–1999 PERIOD

During the first months of 1997 volcanic activity at Mt Etna remained at low levels. It started increasing in July when pyroclastic cones began to form inside Bocca Nuova (BN; Fig. 4), lava began to spill from the Southeast Crater (SEC; Fig. 4) rim and the Voragine (VOR; Fig. 4) and the Northeast Crater (NEC; Fig. 4) started producing mild strombolian activity. During 1998 January, marked fluctuations in the intensity of the activity at BN, SEC and VOR were observed together with a subsidence of the magma column within the BN and the resumption of seismic activity below the western flank of the volcano. During the following months, the activity at the craters stabilized again and the SEC became the focus of the summit activity. During the spring and early summer of 1998 a gradual rise in the activity from all the craters took place. On July 22 a paroxysmal eruptive episode was produced by VOR followed by the first lava flow from the area of the former Central Crater since 1964. It covered the road connecting the northern and southern flanks of Etna. Vigorous activity at BN and SEC occurred simultaneously with the paroxysmal event from VOR, indicating that the episode affected much of the central conduit system at some depth (Smithsonian Institution 1998). The SEC, which had been in nearly continuous activity since 1996 November, remained totally quiet after the event on July 22. On September 15 it reactivated, producing a lava fountaining episode. It was the first of 21 paroxysmal episodes produced by SEC until 1999 February 4. The other summit craters remained quiet during this period. During the previous lava fountaining episode a fracture formed on the SE flank of SEC and lava started flowing from it. While mild explosive activity and vigorous lava emission continued at this new fissure, activity at the other craters gradually ceased. In the summer of 1999 activity from VOR and BN gradually resumed while explosions took place deep inside the NEC conduit. On the fourth of September a strong lava fountain episode was produced by VOR with an eruption column rising ∼2 km high before being blown downwind (Smithsonian Institution 1999). A revival of strombolian activity occurred a few hours after this event at SEC with the formation of a new fracture at the base of the cone, to the north of the previous one, renewing lava emission. Activity at BN became more energetic after the event on September 4 and climaxed with five lava fountaining episodes. As a consequence of this activity, the crater was filled with pyroclastic material and lava overflowed on October 17 producing a lava field extending towards Monte Nunziata (1750 m asl), which crossed the road connecting the northern and southern flanks of Etna. In November the activity from both BN and SEC came to an end.

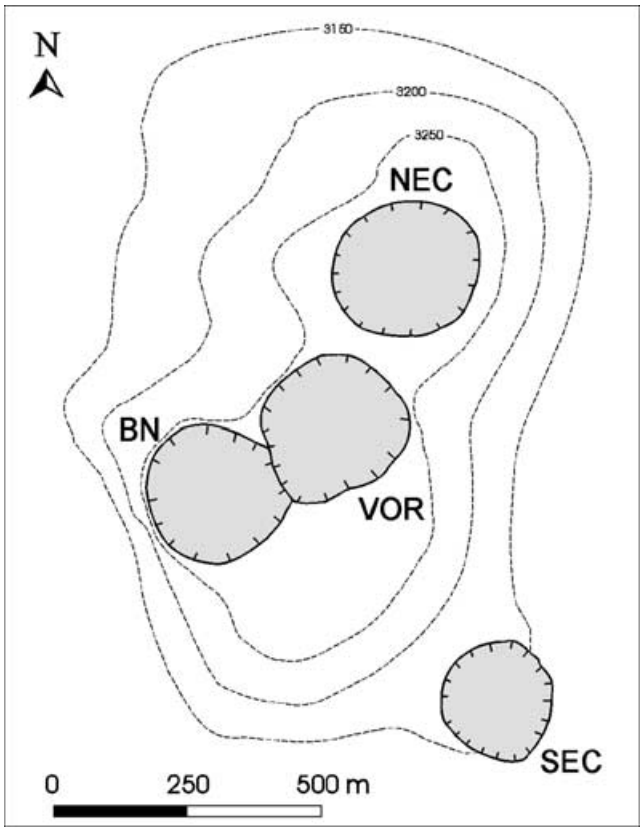

Figure 4. Sketch map of the summit zone of Mt Etna showing the four central craters. BN, Bocca Nuova; NEC, Northeast Crater; SEC, Southeast Crater; VOR, Voragine.

4 DATA PRESENTATION

As stated in Section 2.2, the E–W and summit profiles provide the core microgravity data for Etna. Thus, in the following sections we refer mainly to data from those profiles while data from the remaining stations of the network (surveyed once or twice a year; Section 2.2) are used to better constrain the areal extent of the gravity changes assessed through data from E–W and summit profiles.

4.1 Data from the E–W profile

Variations of gravity with time measured along the E–W profile (Fig. 1) between 1994 August and 1999 September are shown in Fig. 5. The most evident features are (1) the gravity increase starting during the final months of 1995 and culminating at the end of 1996, which was discussed by Budetta *et al.* (1999) and (2) the subsequent gravity decrease continuing until 1999 and bringing the mean value of gravity at each station affected by the change to a lower level than it was in 1994–1995, before the increase took place. Both changes affect mainly the sequences from the eastern limb of the profile and reach the maximum amplitude (+100 and −120 μGal peak-to-peak, respectively) at stations FV4 and CV. It is important to stress that gravity changes at station CH, the closest to the reference station (ADR, approximately 4 km apart), remain within 20 μGal peak-to-peak during the entire period.

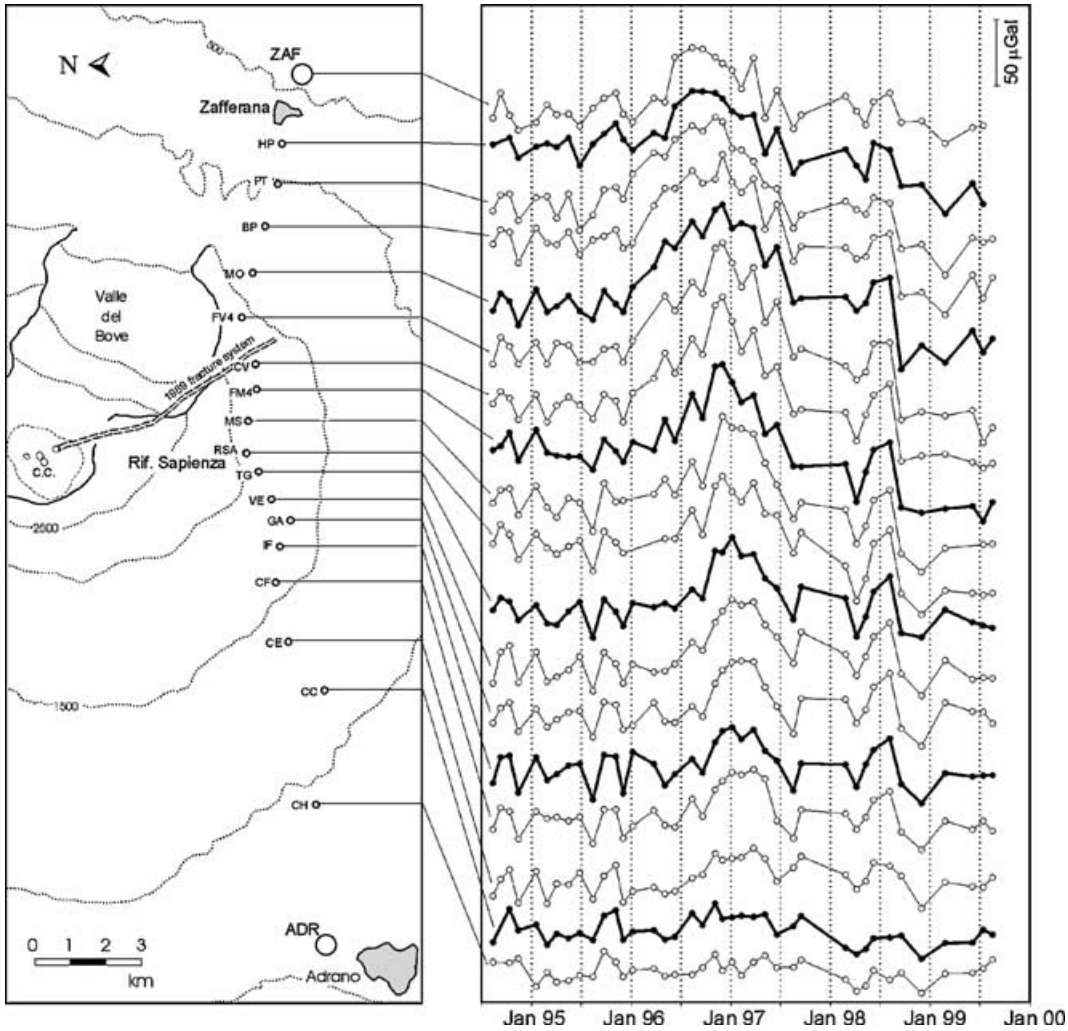

Figure 5. Variation of gravity with time along the E–W profile between 1994 August and 1999 August corrected for the gravity effect of seasonal water-table fluctuations.

Besides the overall changes already presented, other shorter-period changes were observed at the E–W profile stations during the time interval considered. The most significant (being described by four subsequent points) is the increase observed between 1998 April and August (with a maximum amplitude of 40 μGal at station RSA) followed by a sudden decrease between 1998 August and October.

4.2 Data from the summit profile

Gravity changes observed at 16 stations of the summit profile (Fig. 1) between 1994 and 1999 are shown in Fig. 6. Given the inaccessibility of most stations of the profile during the winter time because of snow coverage, all the available points cluster on the June–October period of each year and thus the time resolution of the available sequences is not as good as that of the sequences from the E–W profile stations. Nevertheless, the same increase–decrease cycle already found in the data from the E–W profile is recognizable. However, in the case of data from the summit profile the increase at the very summit stations (from FS to CO) is swamped by the effect of an additional (shallower) source causing a shorter-wavelength (approximately 5 km; centred on the crater zone) and shorter-period (1994 September–1996 July) cycle (Budetta *et al.* 1999). Also, the sequences lack the 1996/97 winter data (apart from the southernmost stations, from CL to PH, which were measured in 1997 November) during which, according to the E–W profile data, the climax of the main cycle took place. So the gravity increase was not recognized by Budetta *et al.* (1999) for the summit profile data. It is noticeable that during the summer of 1997 a step increase was also observed at station SU, one of the closest stations to the summit craters zone, indicating a mass redistribution in the shallowest part of the plumbing system of Etna. Other shorter-period anomalies are superimposed on the general decrease (Fig. 6). The most significant one is the decrease–increase cycle that took place between 1999 June and October and reached 80 μGal peak-to-peak at station LZ (Carbone *et al.* in press). It is noteworthy that, during the summers of 1997 and 1998, measurements at an unusually high rate (weekly to fortnightly) were accomplished along the summit profile (Fig. 6). The standard errors of estimate on the regression lines through these data are between 2 and 15 μGal, in good agreement with the uncertainty of ±11 μGal affecting data from the summit profile (Section 2.2.2).

4.3 Data from the entire Etna network

The entire Etna network (i.e. E–W and summit profiles plus main network; Section 2 and Fig. 1) was measured twice a year until 1997

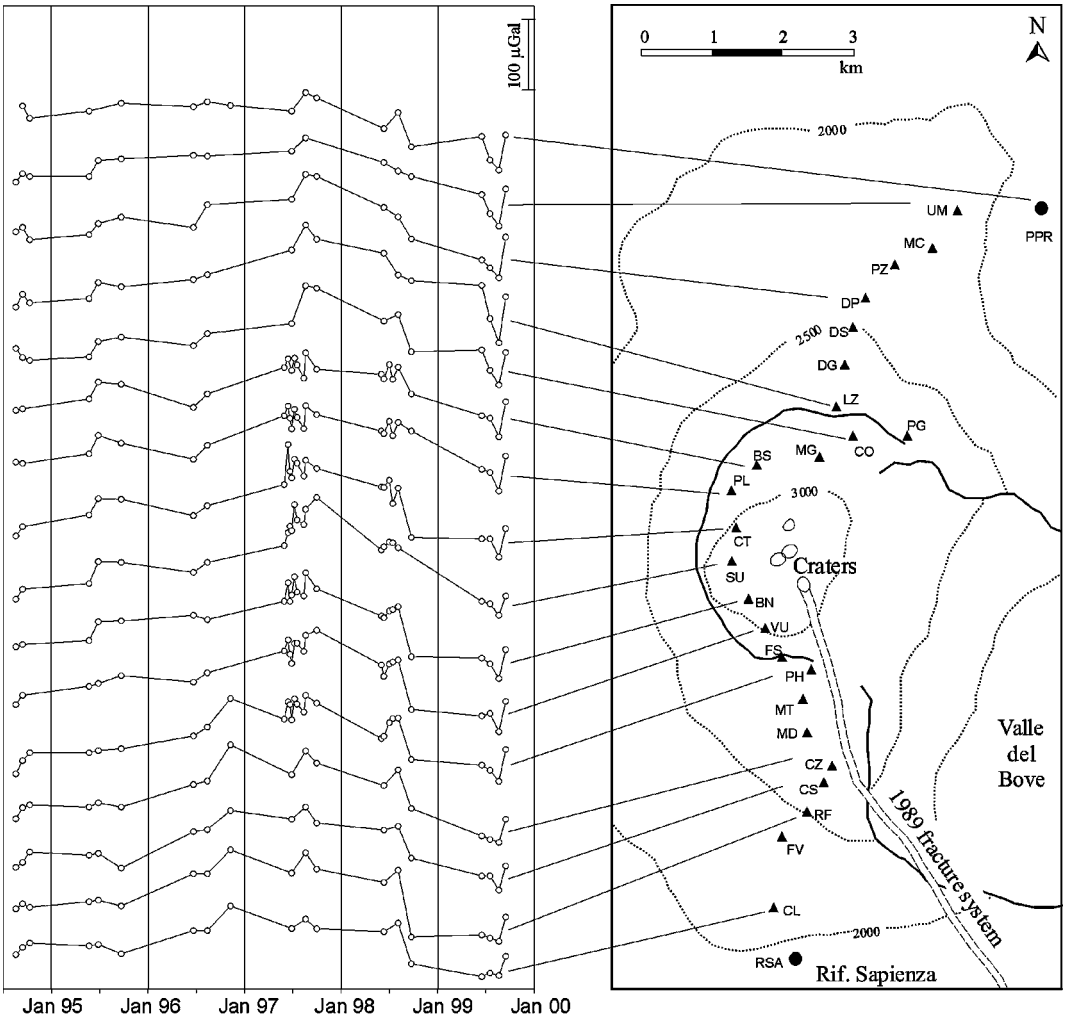

Figure 6. Variation of gravity with time at some stations belonging to the summit profile between 1994 August and 1999 October.

(June–July and September–October) and just once a year in 1998 and 1999. In Fig. 7 contour maps of some gravity changes from the entire Etna network are shown. All maps show only the changes already identified from the E–W and summit profiles stations, indicating an absence of major mass redistributions elsewhere within the gravity network. The second map (Fig. 7b, 1995 October–1996 November) lacks information from the summit stations (between Stations VU and UM, Fig. 1), owing to extensive snow cover in 1996 November. Even so, a wide anomaly corresponding to the gravity increase already described from the profile data is apparent, with a maximum amplitude of approximately 80 μGal (Budetta *et al.* 1999). The gravity decrease discussed above, which took place between the 1996/97 winter and the summer of 1999, also clearly appears in the previous two maps (Figs 7c and d; 1996 November–1997 July and 1997 July–1999 June).

5 POSSIBLE PERTURBATIONS TO THE DATA

5.1 Elevation changes

Besides the redistribution of subsurface masses, changes in surface elevation also cause a gravity change at active volcanoes as the edifice inflates and deflates. Thus gravity and displacement data must be analysed together in order to correctly identify subsurface processes in volcanic areas (Fernández *et al.* 2001). Three basic categories of relationship between gravity and elevation changes can be recognized (Rymer 1996; Budetta & Carbone 1998).

(1) Gravity variations are caused by the inflation or deflation of a shallow magma chamber, as magma is injected or withdrawn. In this case changes in gravity (Δg) and elevation (Δh) are well correlated with a constant value of $\Delta g/\Delta h$ which, for typical densities of basaltic magma, is approximately -233 μGal m^{-1} (Johnsen *et al.* 1980; Torge 1981; Berrino *et al.* 1984; Eggers 1987).

(2) Gravity changes are caused by variations in static magma density (e.g. during degassing), by fluctuations in the level of the water table, or by the injection of magma into previously open dykes. In this case changes in gravity are not accompanied by significant changes in elevation (Sanderson 1982; Rymer *et al.* 1993; Jentzsch *et al.* 2001).

(3) Gravity changes are caused by magma injection or withdrawal coupled with other processes causing a change in bulk density (magma filling and emptying microfractures within a chamber; replacement of relatively low-density summit magma (being erupted or intruded along dykes) by denser magma rising from depth; migration of magma between a chamber and a surrounding porous zone, etc.). In this case Δg and Δh are again well-correlated, but

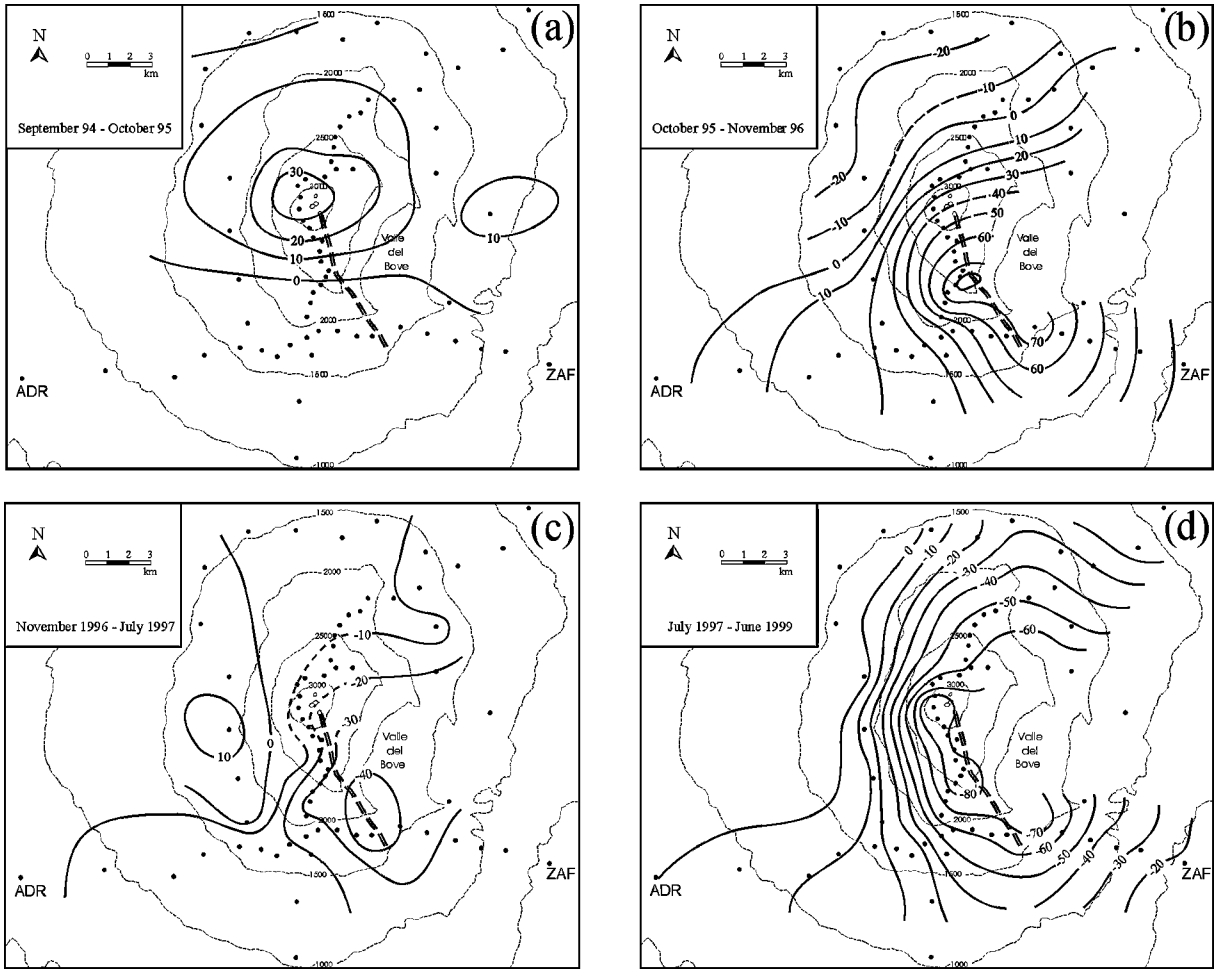

Figure 7. Gravity contour map (at 10 μGal intervals) showing observed gravity changes during the 1994 September–1995 October; 1995 October–1996 November; 1996 November–1997 July and 1997 July–1999 June time intervals. Errors affecting gravity changes are typically within 10 μGal; larger errors affect gravity changes along the summit profile (within 15 μGal).

$\Delta g/\Delta h$ is not usually constant (Dzurisin *et al.* 1980; Jachens & Eaton 1980; Wong & Walsh 1991; Battaglia *et al.* 1999; Rymer & Williams-Jones 2000).

The elevation of each gravity station is not systematically monitored during the gravity surveys. Nevertheless, independent ground-deformation surveys provide enough data to evaluate the vertical deformation of Etna to a detail suitable for our purposes. As for the changes observed during the 1994–1996 period, a maximum elevation effect of approximately 12 μGal, within the normal error in assessing a gravity change (Section 2.2.2), was determined by Budetta *et al.* (1999) using both levelling (Obrizzo 1995, 1996) and GPS (Puglisi & Bonforte 1999) data.

Only GPS data are available to evaluate the gravity effect of elevation changes between 1996 and 1998. During the 1996–1998 period three GPS surveys (1996 July; 1997 June and 1998 June) were carried out along a network of 48 benchmarks most of which coincide or are very close to gravity stations (Puglisi *et al.* 1998). Trimble receivers model 4000 SSE and SSI were used. Data processing was performed through the GPSurvey software package version 2.3, produced by Trimble. Precise ephermerides, computed by the National Geodetic Survey, were also used in order to improve the accuracy of the solutions (Puglisi & Bonforte 1999). The standard deviation affecting changes in the horizontal component ranges between 0.2 and 0.5 cm while, over changes in the vertical component, the standard deviation ranges between 0.3 and 1 cm. Thus, a maximum uncertainty of ± 1 and ± 2 cm at the 95 per cent confidence interval can be assumed over the horizontal and vertical component, respectively.

Between the summers of 1996 and 1997 a general uplift of the area covered by the gravity network took place (Puglisi & Bonforte 1999). This uplift reaches 5–6 cm over the summit zone of the volcano, to the west at a station very close to NZ (Fig. 1) and over the northeastern sector (station RE zone; Fig. 1). Over the following 12 months just a weak lowering was observed over the western sector of Etna. It increases towards the outer zone of the volcano and reaches approximately 5 cm at the very limit of the zone covered by the gravity network (Puglisi & Bonforte 1999).

The GPS network was not surveyed during 1999 and so it is not possible to say whether elevation changes took place during the 1998–1999 period, when the final part of the gravity decrease semi-cycle took place.

Elevation changes observed at the GPS stations coinciding with E–W profile gravity stations during the 1996–1998 period were typically within the error bar of ± 2 cm and reached 4 cm between the summers of 1996 and 1997. Elevation changes recorded at GPS stations coinciding with the summit profile gravity stations (and with the other stations of the Etna network) remained stationary to within

5–6 cm. The nominal $\Delta g/\Delta h$ value of -2.33 μGal cm^{-1} implies a maximum gravity change of approximately 9 and 12–14 μGal for E–W and summit profile stations, respectively. In both cases the gravity effect of the observed elevation changes remains within the normal errors affecting gravity changes along these profiles (typically 10 and 15 μGal on gravity differences from the E–W and summit profiles, respectively; see Section 2.2.2).

Thus, the variations in gravity measured during the period covered by the present study seem not to be related to elevation changes. Accordingly, gravity changes were not corrected for elevation changes. This was also the conclusion of Budetta & Carbone (1998) and Budetta *et al.* (1999) for data acquired at the Etna network during the 1987–1992 and 1994–1996 periods, respectively. Similarly, both Sanderson (1982) and Rymer *et al.* (1993, 1995) found that local elevation changes were not important for gravity changes associated with the 1981 and 1991–1993 eruptions of Etna, respectively. Thus, apparently height variations on Etna are too small to significantly affect surface gravity measurements. Accordingly, where adequate elevation data are not available, large gravity changes can be assumed to be the result only of subsurface variations in mass.

5.2 Water-table effects

The gravity effect of seasonal water-table fluctuations at Mt Etna has been investigated by Budetta *et al.* (1999). Given the shortness of the sequences at their disposal (from 1994 August to 1996 November), Budetta *et al.* (1999) were forced to use a polynomial fit to extract the seasonal part of the signal. Data from the western E–W profile stations (from CH to TG; see Fig. 1), the least affected by volcanically induced gravity changes, were averaged and approximated by an eighth-order polynomial fit the Student's *t*-test showed to be significant at the 92 per cent level. The polynomial fit that closely resembled a sinusoidal pattern with a period of 1 yr (late-winter maxima and late-summer minima) and a peak-to-peak amplitude equal to 20 μGal was assumed to represent the gravity effect of water-table fluctuations (Budetta *et al.* 1999).

The longer sequences now available allow suitable filters to be used. Being able to extract a given frequency band from a signal, bandpass filters allow data from all the E–W profile stations to be used (polynomials behave as low-pass filter and thus they prevent data from the higher E–W profile stations, affected by volcanic-related components with period longer than 1 yr, from being used to extract the seasonal part of the signal). The use of the averaged trend from all the stations of the profile makes the result more robust from a statistical point of view. Naturally, it also implies that a unique correction for the water-table effect is defined for all the stations of the E–W profile (Budetta *et al.* 1999, also used the same correction for all the stations). A bandpass filter (Fig. 8; dashed line), with cut-off periods centred around 1 yr (lower-pass frequency equal to 2.15×10^{-3} cycle d^{-1} and higher-pass frequency equal to 3.77×10^{-3} cycle d^{-1}), has been performed over the averaged trend from all the stations of the profile (Fig. 8; dotted line). The result of the above filter is compared with the sinusoidal model proposed by Budetta *et al.* (1999), which was extrapolated over successive data from the E–W profile, assuming that the fluctuation was stationary in time and its amplitude was constant (Fig. 8; continuous line). The sinusoidal model coincides with the bandpass filter output over the first part of the sequence (approximately 1.5 yr). Afterwards the fit between the two curves worsens even though phase shifts never exceed 2–3 months. The explanations for appreciable divergences between the theoretical stationary model and the bandpass-filtered sequence could be that:

(1) it is logical to expect some phase shift in water-table fluctuations since, being a natural phenomenon, they are affected by variables such as changes in rainfall, temporal shifts in the maximum and minimum annual temperature, etc.;

(2) gravity changes not linked to water-table fluctuations with periods close to 1 yr could also have affected the E–W profile stations.

As stated before, the intrinsic advantages of bandpass filters, allowing extraction of the required band regardless of the length of the data sequence, make the result of the above bandpass filter more robust than the model proposed by Budetta *et al.* (1999). Accordingly, the results of the new model are used to correct data from the E–W profile for the gravity effect of water-table fluctuations (Fig. 5). Since the summit profile is normally accessible only from June to October (Section 4.2), the data acquired are not suitable for evaluating the seasonal effect of water-table fluctuations. Accordingly, data from the summit profile are not corrected for this effect. However, the gravity change of approximately 10 μGal expected for the June–October interval on the E–W profile (Fig. 8) can be considered an upper limit on the possible effects of water-table variations on the summit measurements.

6 DISCUSSION

As stated before, a general gravity increase–decrease cycle was observed along the Etna network between 1995 and 1999. The 1995–1996 increase part of the cycle was not recognized at the summit profile stations by Budetta *et al.* (1999) because of swamping by the 1994–1996 local changes at the stations closer to the summit craters and to the lack of 1996–1997 winter data from all but the southernmost stations of the profile. Data from 1997 onwards, now available,

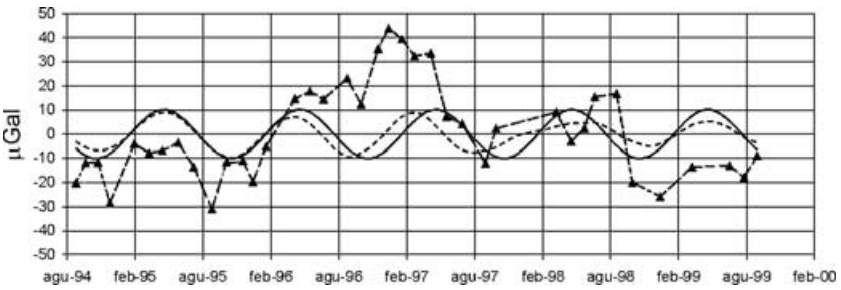

Figure 8. Comparison between the model proposed by Budetta *et al.* (1999) for the gravity effect of water-table fluctuation on Etna (continuous line) and the bandpass filter, with cut-off periods centred around 1 yr (dashed line), performed over the averaged data from all the stations of the E–W profile (dotted line).

suggest that the main 1995–1999 cycle may also have occurred at the summit profile stations (Fig. 6).

The apparent shift in time at the climax of the cycle, which seems to exist if data sequences from E–W and summit profile stations are compared (Figs 5 and 6), could be, at least in part, the effect of the lack of winter 1996/97 data from the summit stations. To illustrate this point, the southernmost summit profile stations (from CL to PH), which were unusually measured in 1996 November, show the climax of the main cycle over that date (Fig. 6). Given the similarity of the increase–decrease 1995–1999 cycles assessed through the sequences from E–W and summit profiles as for overall period and phase, they are likely to be caused by the same source. Thus, the mass centre of the model source calculated by Budetta *et al.* (1999) to explain the 1995–1996 gravity increase on the ground of the data from the E–W profile stations alone is likely to be shifted towards the south with respect to its actual position and also the mass involved in the redistribution phenomenon is likely to be underestimated. To invert the 1997–1999 decrease part of the cycle, both data sets from the E–W and summit profiles are used. The main drawback of doing so is the lack of 1996–1997 winter data from the summit profile, which forces the interval 1997 July–1999 June to be selected to represent contemporary gravity changes along the E–W and summit profiles (1997 July is the first campaign accomplished along the summit profile after the decrease took place). This naturally implies that just 60–70 per cent of the amplitude of the decrease observed along the E–W profile (Fig. 5) will be inverted. However, the advantage of using data from both profiles in order to better constrain the position of the model source and the total mass involved in the redistribution process is evident. In Fig. 9 gravity changes observed during the 1997 July–1999 June period along the E–W and summit profiles are presented. The wider anomaly shows a wavelength of approximately 12 km along the E–W profile (centred on station FV4) and more than 20 km along the summit profile (centred on station SU).

Since it is not possible to assess analytically a unique model from a measured gravity anomaly (or field), to solve the inversion problem the model that is most realistic on geological and geophysical grounds has to be chosen. That means that some limiting *a priori* conditions have to be assumed in order to *guide* the inversion process. For the inversion of the 1997 July–1999 June gravity changes, the following constraints on the model source have been assumed.

6.1 Mass change

The total mass involved in a redistribution process can be uniquely determined without any assumption whatsoever regarding shape, density change or depth of the source body. The basis of the calculation is a Gaussian surface integration of the residual anomaly over the area of measurement (Sharma 1986). The formula giving the total mass (in metric tons) is (Grant & West 1965)

$$M = \frac{1}{2\pi G}\int\int_s \Delta g(x, y)\, dx\, dy \tag{1}$$

$$= 2.39 \sum \Delta g \times \Delta S, \tag{2}$$

where Δg is the mean anomaly (gravity change, in the case of the present study, in mGal) within a small area element ΔS (m^2) and $\sum \Delta g \times \Delta s$ is the summation over the whole measurement area. Since only the order of magnitude of the 1997–1999 mass change is needed at this stage to define the edge values for the range to be investigated, the term $\sum \Delta g \times \Delta S$ in eq. (2) can be replaced by the area within the zero contour line in Fig. 7(d) multiplied by the mean gravity change occurring within it. Comparing Figs 7(d) and 9, one can argue that reasonable values for these two variables are 3.25 ×

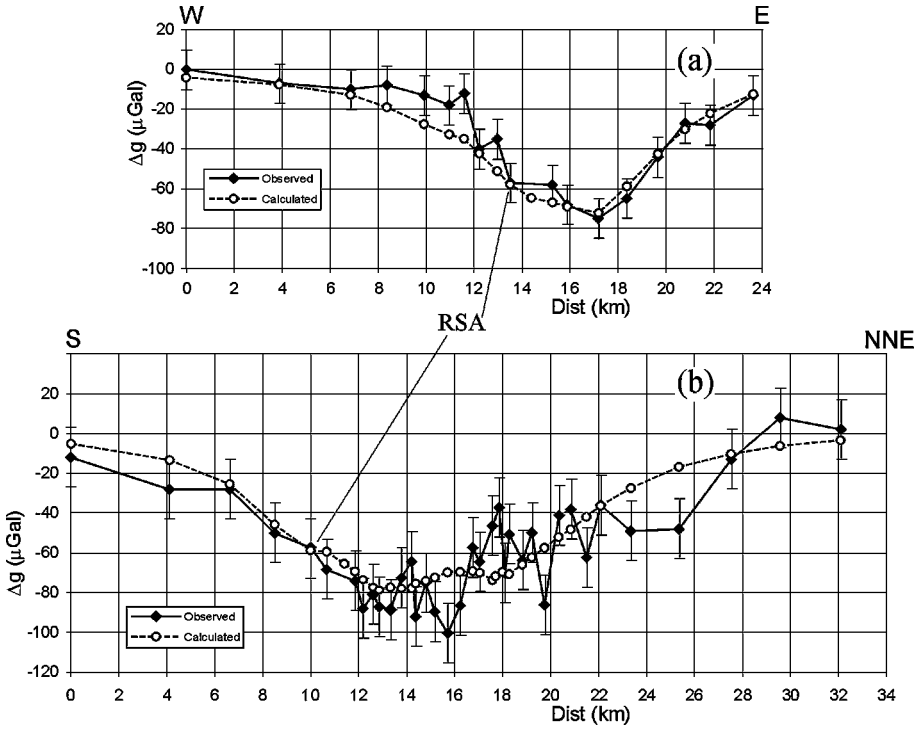

Figure 9. Gravity changes observed along the E–W (a) and summit (b) profiles during the 1997 July–1999 June period and the gravity effect of the best-fitting model source (see text for details). The position of station RSA, common to both profiles, is indicated. Errors affecting gravity changes along the E–W profile are typically within 10 μGal, whereas those on changes from the summit profile are typically within 15 μGal.

10^9 m^2 and 0.05 mGal. The corresponding mass change thus equals approximately 4×10^8 metric tons, i.e. 4×10^{11} kg.

6.2 Shape

The extensional stress regime beneath Etna is thought to allow the ascent of magma from the asthenospheric source (Continisio *et al.* 1997; Cristofolini *et al.* 1987). Magma batches that accumulate episodically beneath the volcano are thus likely to be lens-shaped, especially if a model of magma movement by fracture propagation is assumed (Shaw 1980). Such a geometry can be approximated by a prism and has already been used to interpret mass changes detected below the base of the volcano (Budetta & Carbone 1998; Budetta *et al.* 1999).

6.3 Azimuth

As shown in Fig. 7(d) the 1997 July–1999 June gravity change is centred on the southeastern sector of the volcano. The major structural trend located in that sector is that oriented NNW–SSE (Lo Giudice & Rasà 1986; Lo Giudice & Rasá 1992), which is thought to be a preferred alignment for the ascent of Etnean magmas (Continisio *et al.* 1997) especially for activity since 1989 (Ferrucci *et al.* 1993; Alparone *et al.* 1994; Bonaccorso *et al.* 1994; Budetta & Carbone 1998).

6.4 Depth of the mass centre

Magma accumulations have been found at different levels within the crust under Etna by several geophysical techniques. In general, the shallower zones of magma accumulation have been found to lie at depths between 1.5 and 5 km bsl (Bonaccorso *et al.* 1994; Nunnari & Puglisi 1994; Bonaccorso 1996; Budetta & Carbone 1998; Murru *et al.* 1999). Deeper zones of magma accumulation are thought to lie at approximately 10 km bsl (Lanari *et al.* 1998; Murru *et al.* 1999), but their possible gravity effect would cover a distance greater than the total extent of our network and thus would be beyond the limits of detection by the gravity surveys.

The kernel of a 3-D computer program named GRAVERSE (Carbone 2001), which automatically calculates the effect of a prism-shaped model source over a range of values set by the operator for each sensitive parameter has been utilized. In particular, following the above conditions, the range of depths for the model mass centre has been set to 1500–5000 m bsl (increment of 500 m), whereas the range for the azimuths of the elongated body has been set to 360–315°N (increment = 15°). The total mass of the body has been allowed to range between 2.5 and 6×10^{11} kg. This means that, since the vertical extent, the thickness and the density change are not sensitive parameters, their product has been fixed to 5×10^7 kg m^{-1}, whereas the length of the body (i.e. the only sensitive parameter affecting the total mass) has been allowed to range between 5000 and 12 000 m (increment of 1000 m).

The above ranges for each sensitive parameter are summarized in Table 1.

Table 1. Ranges for each sensitive parameter of the source model to be calculated.

Parameter	Start value	End value	Increment
Length	5000 m	12 000 m	1000 m
Mass centre depth	1500 m bsl	5000 m bsl	500 m
Azimuth	360°N	315°N	15°

As for the position of the source model in the horizontal plane, based on the shape of the anomaly (Fig. 7d), the projection of the mass centre has been assumed to lie on the southeastern sector of the volcano, strictly on one of the nodes of a square grid (side length of 10 km) the bottom left vertices of which coincides with the RSA station (Fig. 1) and where the node spacing is equal to 500 m.

The above degrees of freedom involved in the choice of the model used to invert the 1997 July–1999 June gravity change required nearly 113 000 iterations by GRAVERSE. For each model tried the program automatically calculates the standard error of the estimate (s_{xy} in μGal):

$$S_{xy} = \sqrt{\frac{\sum (Y_{\text{obs}} - Y_{\text{est}})^2}{N}}, \tag{3}$$

where Y_{obs} is the gravity change observed at a given station during the 1997 July–1999 June period, Y_{est} is the effect of each model source calculated at the same station by the program, whereas N is the total number of stations used for the inversion process.

The result of the above calculation is shown in Fig. 10 where the s_{xy} statistic, corresponding to each model tried is reported. It must be stressed that to make the chart easier to be read only models giving $s_{xy} \leq 50$ have been reported (the maximum s_{xy} value obtained was 84). The points in the chart cluster in different fields are separated by vertical lines: thick lines separate models with a different length (and thus total mass), while thin lines separate, within each class of length, models at different depths. Within each class of depth, four different classes of azimuth are comprised (lines have been reported only on the very first sector). As stated before for each model of given length, depth and azimuth, 441 positions on the horizontal plane were tried.

Fig. 10 also shows that the longer the source model is (and thus the greater the total mass), the deeper it must be to better fit the observed change (the minimum s_{xy} occurs closer and closer to the right-hand edge of each length field as the length of the model source increases). As one can easily see, a pronounced minimum does not exist (the minimum s_{xy} ranges between 13.3 and 14.3 μGal for models with lengths ranging between 8000 and 12 000 m). However, since no independent estimate can be made of the amount of matter to be removed within the volcano, the model giving the absolute minimum s_{xy} is chosen. The characteristics of this model, which gives $s_{xy} =$ 13.3 μGal, are reported in Table 2. The mass change inferred is approximately 5×10^{11} kg.

To assess the quality of the model source a paired t-test has been performed. This tests the hypothesis that the mean of the differences between the observed gravity change and the corresponding calculated effect of the model source at each station is equal to zero. The p-value obtained (0.88) indicates that is likely (a chance of 88 in 100) that the hypothesized zero mean difference would occur by chance. The absence of a statistically significant difference between the observed and calculated gravity changes confirms the effectiveness of the best model source.

In Fig. 9 the effect of the best-fitting model source is presented and compared with the gravity changes observed along the E–W and summit profiles between 1997 July and 1999 June. The values of s_{xy} relative to the E–W and summit profiles data (9.5 and

Table 2. Best model source parameters. The origin of the coordinate system is coincident with RSA station (Lat. N = 37°42′ 00″; Long. E = 14°59′ 54″; Fig. 1).

X centre (m)	Y centre (m)	Z centre (m bsl)	Length (m)	Azimuth (°N)
1000	4500	3500	10 000	330

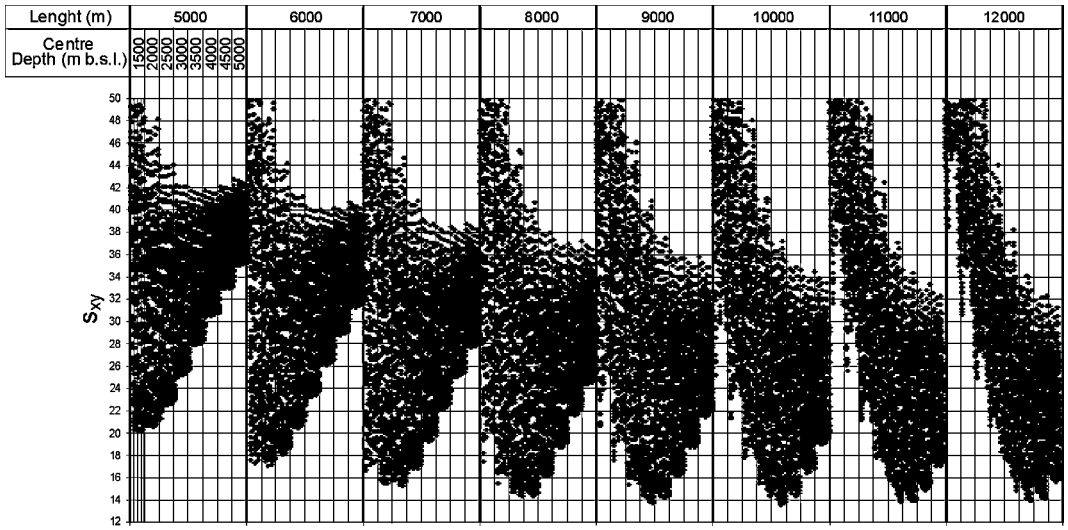

Figure 10. s_{xy} statistic (standard error of the estimate) corresponding to each of the nearly 113 000 models automatically tried to fit the 1997 July–1999 July gravity changes (see text). Bold vertical lines separate points corresponding to models with different length (values reported in the very upper field); thin vertical lines separate models at different depth (only values corresponding to the first class of length have been reported). In the very first sector, lines separating models with different azimuth have been also drawn (values, not reported, are 360°N, 345°N, 330°N and 315°N).

15.2 μGal, respectively) are very close to the errors typically affecting changes along those profiles (10 and 15 μGal, respectively; Budetta *et al.* 1999).

The projection on to the surface of the above best-fitting model source is shown in Fig. 11 together with the projection on to the surface of the model source calculated by Budetta *et al.* (1999) to explain the 1995–1996 gravity increase. The model source calculated to invert the 1997 July–1999 June gravity decrease is larger than that calculated to explain the previous increase, with its southern tip overlapping the smaller source model. In fact, because of the reasons stated at the beginning of the present section, only data from the E–W profile were used for the inversion of the 1995–1996 gravity increase and thus just part of the entire source could have been detected by Budetta *et al.* (1999). As stated previously, this could imply that more mass than Budetta *et al.* (1999) calculated (1.5×10^{11} kg) could have entered the basement of the volcano between 1995 October and 1996 November (the mass associated with the 1997 July–1999 June gravity decrease through the above calculation is approximately three times larger than the mass associated by Budetta *et al.* (1999) with the previous increase, in spite of the comparable amplitude of the two semi-cycles; Figs 5 and 6). Finally, it should be stressed that the centre of the above calculated best-fitting model source is approximately 1 km deeper than the magma body postulated by (Budetta *et al.* 1999, Fig. 11).

7 CONCLUSIONS

The calculation performed in the above section shows that a mass decrease of approximately 5×10^{11} kg took place between 1997 July and 1999 June within an elongated volume 3–4 km bsl deep, oriented NNW–SSE and with its mass centre approximately 2 km SSE of the summit craters. For a large amount of matter to be removed without appreciable elevation changes (Puglisi & Bonforte 1999, see Section 5.1), either a density change must have occurred in a pre-existing magma body or magma movements must have taken place. Previous gravity measurements have shown that significant amounts of magma have been accommodated within the same accumulation zone (Budetta & Carbone 1998; Budetta *et al.* 1999). Thus, this zone is likely to be a preferred reservoir for magma rising from deeper sources. The most important mechanism allowing the density of a static magma body to sensibly decrease is gas exsolution (Rymer & Brown 1987). In general, a decrease of pressure within a magma body causes a simple gas law expansion of vesicles on one hand and a decrease in solubility of the volatile component on the other. Both effects result in a net density decrease as shown at the Poas and Masaya volcanoes by Rymer *et al.* (1998, 2000).

The principal gases present in Etnean magmas are H_2O, CO_2 and SO_2. The study of melt inclusions trapped in phenocrysts, matrix glasses and whole rocks indicates the volatile abundance of the Etna primitive basalts to be at approximately 1.5 wt per cent for H_2O and 0.3 wt per cent for both CO_2 and SO_2 (Metrich & Mosbah 1988; Metrich *et al.* 1993). The solubility of H_2O and SO_2 in magma is much greater than that of CO_2 and thus, although water dominates shallow strombolian activity, CO_2 is the main volatile at greater depths. In general, the temperature dependence on volatile solubility is negligible, whilst pressure and initial concentration are key factors (Wilson & Head 1981). For the above abundances a boiling depth of approximately 3 km below the surface (∼100 MPa) has been proposed (Kadik & Lukanin 1973; Wilson & Head 1981).

As shown in Fig. 11, the best-fitting model source calculated in the previous section lies below the minimum depth at which gas exsolution, corresponding to the above reported abundances, starts occurring.

A more realistic model, involving non-vesicular magma, is based on the control that extensional tectonic stresses, acting on the lithosphere of eastern Sicily (Cristofolini *et al.* 1987; Bousquet *et al.* 1988), exercise on magma rising from the deep-seated mantle source.

At Mt Etna magma is thought to rise from the asthenospheric source through a plexus of molten lenses within the lithosphere behaving as a porous medium (Hill 1977; Shaw 1980). Following this view, the amount of molten material within these porous zones is controlled by extensional tectonic stresses and thus, given the density contrast between magma and host rock, tectonic stresses also control the density changes occurring within these volumes.

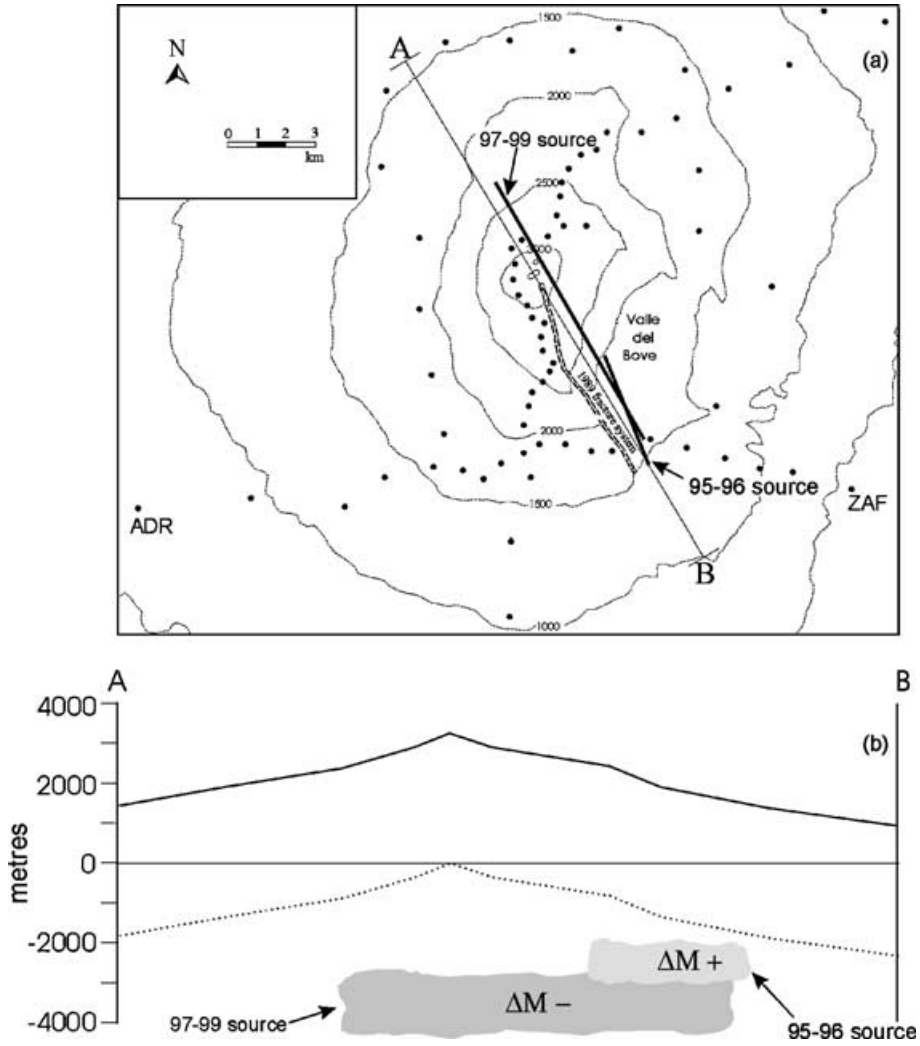

Figure 11. The gravity decrease occurred at Mt Etna between 1997 and 1999 has been attributed to a density change in a prism-shaped source-body where the projection on to the surface is shown in (a) and where the projection on to a NNW–SSE cross-section (AB) is shown in (b). The projection on to the surface and the same cross-section of the model-source postulated by Budetta *et al.* (1999) are also reported. The dashed line in (b) marks the depth at which etnean magmas start exsolving gases (see the text for details).

Regional stresses deforming the lithosphere could have a very small effect on the volcanic edifice (i.e. no significant deformation), owing to attenuation by: (1) concentrated deformation along a failure plane below Etna between the Apennine–Maghrebide Chain and the Iblean Plateau (Lentini *et al.* 1995), (2) slippage between the nappes of the Apennine–Maghrebide Chain and (3) fracturing near the base of the volcanic pile (McGuire & Pullen 1989).

Our data indicate that between 1997 and 1999 the magma previously accumulated within the inferred model source volume (or just a part of it) migrated. Some of the escaping magma could have entered the shallower part of the plumbing system of Etna, giving rise to the subsequent explosive activity that culminated during the spring and early summer of 1998 (Section 3). Consistent with this view are: (1) the gradual increase in the strain release from 1996 July until the beginning of 1999 (Bonaccorso & Patanè 2001; La Delfa *et al.* 2001); (2) a large increase in the tremor amplitude in 1998–1999 (La Delfa *et al.* 2001) and (3) the emission of primitive and gas-rich magma from depth (La Delfa *et al.* 2001) in 1998 (VOR and BN; Fig. 4) and in 1999 (SEC; Fig. 4).

The model proposed above implies a volume of lost magma given by $\Delta M/(\rho_m - \rho_r)$, where ΔM is the observed change in mass, ρ_m is the density of new magma and ρ_r is the density of the host rock (Budetta & Carbone 1998). Using the empirical relation of Nafe & Drake (1963), seismic tomographic data for Etna (Cardaci *et al.* 1993) indicate a mean host rock density of approximately 2300 kg m^{-3} at 3–4 km below sea level. Assuming a density of 2800 kg m^{-3} for non-vesicular basic magma, the volume of magma corresponding to the mass lost from the inferred source zone within the volcano is approximately 10^9 m^3.

Measurements of SO_2 flux indicate approximately 2–4 $\times$ 10^8 m^3 of magma exsolving SO_2 (and thus entering the shallower part of the Etna plumbing system at depths less than 2–3 km below the surface) each year (Allard 1997; Bruno *et al.* 1999). Thus, at one extreme, nearly all the magma lost from the 3–4 km deep reservoir during the 1997–1999 period could have entered the shallower part of the plumbing system of Etna. This would imply the absence of any replenishment from deeper zones during the above period. However, it should be stressed that, according to the calculations performed by Allard (1997), Bruno *et al.* (1999) and Harris *et al.* (2000), only approximately 10 per cent of the basalt that contributes the SO_2 emission at Etna has erupted. The unerupted degassed magma is thought to sink down into the magma column and be recycled in

subedifice feeders (Allard 1997). For the density in the 3–4 km bsl deep accumulation zone to decrease, the descending flux must have sunk down to greater depths. Accordingly, Allard (1997) proposes the 'plutonic' complex approximately 10 km wide and deep, detected within the sedimentary basement of Etna (Hirn *et al.* 1991, 1997; Borgia *et al.* 1992; Mauriello *et al.* 1997), to be the final destination for the unerupted magma that thus contributes to the accretion of wide plutonic roots in the basement of Etna.

Also, since significant anomalies have not been observed at the summit stations, the rising to sinking magma budget (i.e. the total mass) along the shallower part of the plumbing system of Etna (from the 3–4 km bsl deep accumulation zone upward) must have remained almost balanced during the 1997–1999 period. This means that the mass decrease at the inferred accumulation zone is the result of a decrease in the number of magma batches coming from deeper zones. Sudden breaks to the equilibrium in the upper part of the feeder system of Etna (i.e. a large amount of magma suddenly entering the volcanic pile without the system being able to recycle it), which would be detected by our network, could lead to system instability and, possibly, large flank eruptions.

ACKNOWLEDGMENTS

The authors thank both Dr G. Williams-Jones and Dr G. Jentzsch for their helpful suggestions.

REFERENCES

AGIP, 1976. Carta gravimetrica della Sicilia.

Allard, P., 1997. Endogenous magma degassing and storage at Mount Etna, *Geophys. Res. Lett.,* **24,** 2219–2222.

Alparone, S., Pellicori, O., Ursino, A., Ferrucci, F., Gresta, S. & Guerra, I., 1994. Shallow microseismic swarms and intrusive mechanisms at Mt Etna, *Acta Vulcanol.,* **4,** 75–79.

Battaglia, M., Roberts, C. & Segall, P., 1999. Magma intrusion beneath Long Valley caldera confirmed by temporal changes in gravity, *Science,* **285,** 2119–2122.

Berrino, G., Corrado, G., Luongo, G. & Toro, B., 1984. Ground deformation and gravity changes accompanying the 1982 Pozzuoli uplift, *Bull. Volcanol.,* **47,** 187–200.

Berrino, G., Rymer, H., Brown, G.C. & Corrado, G., 1992. Gravity–height correlations for unrest at calderas, *J. Volc. Geotherm. Res.,* **53,** 11–26.

Bonaccorso, A., 1996. Dynamic inversion of ground deformation data for modelling volcanic sources (Etna 1991–1993), *Geophys. Res. Lett.,* **25,** 451–454.

Bonaccorso, A. & Patanè, D., 2001. Shear response to an intrusive episode at Mt Etna volcano (January 1998) inferred through seismic and tilt data, *Tectonophysics,* **334,** 61–75.

Bonaccorso, A., Velardita, R. & Villari, L., 1994. Ground deformation modeling of geodynamic activity associated with the 1991–1993 Etna eruption, *Acta Vulcanol.,* **4,** 87–96.

Borgia, A., Ferrari, L. & Pasquarè, G., 1992. Importance of gravitational spreading in the tectonic and volcanic evolution of Mount Etna, *Nature,* **37,** 231–235.

Bousquet, J.C., Lanzafame, G. & Paquin, C., 1988. Tectonics, stress and volcanism: in situ stress measurement and neotectonic investigations in the Etna area (Italy), *Tectonophysics,* **149,** 219–231.

Bruno, N., Caltabiano, T. & Romano, R., 1999. SO_2 emissions at Mt Etna with particular reference to the period 1993–1995, *Bull. Volcanol.,* **60,** 405–411.

Budetta, G. & Carbone, D., 1997. Potential application of the Scintrex CG-3M gravimeter for monitoring volcanic activity: results of field trials on Mt Etna, Sicily, *J. Volc. Geotherm. Res.,* **66,** 199–214.

Budetta, G. & Carbone, D., 1998. Temporal variations in gravity at Mt Etna (Italy) associated with the 1989 and 1991 eruptions, *Bull. Volcanol.,* **59,** 311–326.

Budetta, G., Grimaldi, M. & Luongo, G., 1989. Variazioni di gravità nell'area etnea (1986–1989), *Boll. GNV,* **5,** 137–146.

Budetta, G., Carbone, D. & Greco, F., 1999. Subsurface mass redistribution at Mount Etna (Italy) during the 1995–1996 explosive activity detected by microgravity studies, *Geophys. J. Int.,* **138,** 77–88.

Carbone, D., 2001. Gravity monitoring of Mount Etna (Italy) through discrete and continuous measurements, *PhD thesis*, The Open University, Milton Keynes.

Carbone, D. & Rymer, H., 1999. Calibration shifts in a LaCoste-and-Romberg gravimeter: comparison with a Scintrex CG-3M, *Geophys. Prospect.,* **47,** 73–83.

Carbone, D., Budetta, G., Greco, F. & Rymer H. Combined discrete and continuous gravity observations at Mt Etna, *J. Volc. Geotherm. Res.,* in press.

Cardaci, C., Coviello, M., Lombardo, G., Patanè, G. & Scarpa, R., 1993. Seismic tomography of Etna volcano, *J. Volc. Geotherm. Res.,* **56,** 357–368.

Continisio, R., Ferrucci, F., Gaudiosi, G., Lo Bascio, D. & Ventura, G., 1997. Malta escarpment and Mt Etna: early stages of an asymmetric rifting process? Evidences from geophysical and geological data, *Acta Vulcanol.,* **9,** 45–53.

Cristofolini, R., Gresta, S., Imposa, S., Menza, S. & Patanè, G., 1987. An approach to problems on energy sources at Mt Etna from seismological and volcanological data, *Bull. Volcanol.,* **49,** 729–736.

Dzurisin, D. *et al.*, 1980. Geophysical observations of Kilauea volcano, Hawaii, 2. Constraints on the magma supply during November 1975–September 1977, *J. Volc. Geotherm. Res.,* **7,** 241–269.

Eggers, A.A., 1983. Temporal gravity and elevation changes at Pacaya volcano, Guatemala, *J. Volc. Geotherm. Res.,* **19,** 223–237.

Eggers, A.A., 1987. Residual gravity changes and eruption magnitudes. *J. Volc. Geotherm. Res.,* **33,** 201–216.

Fernández, J., Charco, M., Tiampo, K.F., Jentzsch, G. & Rundle, J.B., 2001. Joint interpretation of displacement and gravity data in volcanic areas. A test example: Long Valley Caldera, *Geophys. Res. Lett.,* **28,** 1063–1066.

Ferrucci, F., Rasà, R., Gaudiosi, G., Azzaro, R. & Imposa, S., 1993. Mt Etna: a model for the 1989 eruption, *J. Volc. Geotherm. Res.,* **56,** 35–56.

Grant, F.S. & West, G.F., 1965. *Interpretation Theory in Applied Geophysics,* McGraw-Hill, New York.

Harris, A.J.L., Murray, J.B., Aries, S.E., Davies, M.A., Flynn, L.P., Wooster, M.J., Wright, R. & Rothery, D.A., 2000. Effusion rate trends at Etna and Krafla and their implications for eruptive mechanisms, *J. Volc. Geotherm. Res.,* **102,** 237–270.

Hill, D.P., 1977. A model for earthquake swarms, *J. geophys. Res.,* **82,** 1347–1352.

Hirn, A., Nercessian, A., Sapin, M., Ferrucci, F. & Wittlinger, G., 1991. Seismic heterogeneity of Mt Etna: structure and activity, *Geophys. J. Int.,* **105,** 139–153.

Hirn, A., Nicolich R., Gallart, J., Laigle, M., Cernobori, L. & ETNASEIS Scientific Group, 1997. Roots of Etna volcano in faults of great earthquakes, *Earth planet. Sci. Lett.,* **148,** 171–191.

Jachens, R.C. & Eaton, G.P., 1980. Geophysical observations of Kilauea volcano, Hawaii, 1. Temporal gravity variations related to the 29 November, 1975, $M = 7.2$ earthquake and associated summit collapse, *J. Volc. Geotherm. Res.,* **7,** 225–240.

Jentzsch, G., Punongbayan, R.S., Schreiber, U., Seeber, G., Völksen, C. & Weise, A., 2001. Mayon volcano, Philippines: changes of monitoring strategy after microgravity and GPS measurement from 1992 to 1996, *J. Volc. Geotherm. Res.,* **109,** 219–234.

Johnsen, G.V., Bjornson, A. & Sigurdsson, S., 1980. Gravity and elevation changes caused by magma movement beneath Krafla caldera, northwest Iceland, *J. Geophys.,* **47,** 132–140.

Kadik, A.A. & Lukanin, O.A., 1973. The solubility-dependent behaviour of water and carbon dioxide in magmatic processes, *Geochem. Int.,* **10,** 115–129.

La Delfa, S., Patanè, G., Clocchiatti, R. Joron, J.-L. & Tanguy J.-C., 2001. Activity of Mount Etna preceding the February 1999 fissure eruption: inferred mechanism from seismological and geochemical data, *J. Volc. Geotherm. Res.,* **105,** 121–139.

Lanari, R., Lundgren, P. & Sansosti, E., 1998. Dynamic deformation of Etna volcano observed by satellite radar interferometry, *Geophys. Res. Lett.,* **25,** 1541–1544.

Lentini, F., Carbone, S., Catalano, S., Di Stefano, A., Gargano, C., Romeo, M., Strazzulla, S. & Vinci, G., 1995. Sedimentary evolution of basins in mobile belts: examples from the Tertiary terrigenous sequences of the Peloritani Mountains (NE Sicily), *TerraNova,* **7,** 161–170.

Lo Giudice, E. & Rasà, R., 1986. The role of the NNW structural trend in the recent geodynamic evolution of North-Eastern Sicily and its volcanic implications in the Etnean area, *J. Geodyn.,* **5,** 309–330.

Lo Giudice, E. & Rasá, R., 1992. Very shallow earthquakes and brittle deformation in active volcanic areas: the etnean region as exsample, *Tectonophysics,* **202,** 257–268.

Mauriello, P., Patella, D., Petrillo, Z. & Siniscalchi, A., 1997. Mount Etna structural exploration by magnetotellurics, *Acta Vulcanol.,* **9,** 141–146.

McGuire W.J. & Pullen A.D., 1989. Location and orientation of eruptive fissures and feeder-dykes at Mount Etna; influence of gravitational and regional tectonic stress regimes, *J. Volc. Geotherm. Res.,* **38,** 325–344.

Metrich, N. & Mosbah, M., 1988. Carbon content of some basaltic glasses: nuclear microprobe analysis, *Bull. Mineral.,* **111,** 511–522.

Metrich, N., Clocchiatti, R., Mosbah, M. & Chaussidon, M., 1993. The 1989–1990 activity of Etna magma mingling and ascent of H_2O–Cl-S rich basalt magma. Evidence from melt inclusions, *J. Volc. Geotherm. Res.,* **59,** 131–144.

Murru, M., Montuori, C., Wyss, M. & Privitera, E., 1999. The locations of magma chambers at Mt Etna, Italy, mapped by *b*-values, *Geophys. Res. Lett.,* **26,** 2553–2556.

Nafe, J.E. & Drake, C.L., 1963. Physical properties of marine sediments, in *The Sea,* Vol. 3, pp. 794–815, ed. Hill, M.N., Interscience, New York.

Nunnari, G. & Puglisi, G., 1994. The Global Positioning System as a useful technique for measuring ground deformations in volcanic areas, *J. Volc. Geotherm. Res.,* **61,** 267–280.

Obrizzo, F., 1995. Monte Etna—movimenti verticali del suolo, *Rep. Osservatorio Vesuviano,* Napoli.

Obrizzo, F., 1996. Monte Etna—movimenti verticali del suolo, *Rep. Osservatorio Vesuviano,* Napoli.

Puglisi, G. & Bonforte, A., 1999. Monitoring active deformation of volcanoes by interferometry as an early warning system, in *MADVIEWS, EC Project n. ENV4-CT96–0294*, *Contribution of CNR – IIV, Final Report*.

Puglisi, G. *et al.*, 1998. GPS measurements: improvements in network configuration and surveying techniques, in *Data Related to Eruptive Activity, Unrest Phenomena and Other Observations on the Italian Active Volcanoes. Geophysical Monitoring of the Italian Active Volcanoes 1993–1995—Etna—Ground Deformation Monitoring,* Vol. 10, pp. 158–169, ed. Gasperini, P., Acta Volcanol.

Rymer, H., 1989. A contribution to precision microgravity data analysis using LaCoste and Romberg gravity meters, *Geophys. J.,* **97,** 311–322.

Rymer, H., 1996. Microgravity monitoring, in *Monitoring and Mitigation of Volcanic Hazards,* pp. 169–197, eds Scarpa, R. & Tilling, R.I., Springer, Berlin.

Rymer, H. & Brown, G.C., 1987. Causes of Microgravity change at Poás volcano, Costa Rica: an active but non-erupting system, *Bull. Volcanol.,* **49,** 389–398.

Rymer, H. & Williams-Jones, G., 2000. Volcanic eruption prediction: magma chamber physics from gravity and deformation measurements, *Geophys. Res. Lett.,* **27,** 2389–2392.

Rymer, H., Murray, J.B., Brown, G.C., Ferrucci, F. & McGuire, J., 1993. Mechanisms of magma eruption and emplacement at Mt Etna between 1989 and 1992, *Nature,* **361,** 439–441.

Rymer, H., Cassidy, J., Locke, C.A. & Murray, J.B., 1995. Magma movements in Etna volcano associated with the major 1991–1993 lava eruption: evidence from gravity and deformation, *Bull. Volcanol.,* **57,** 451–461.

Rymer, H., van Wyk de Vries, B., Stix, J. & Williams-Jones, G., 1998. Pit crater structure and processess governing persistent activity at Masaya volcano, Nicaragua, *Bull. Volcanol.,* **59,** 345–355.

Rymer, H., Cassady, J., Locke, C.A., Barboza, M.V., Barquero, J., Brenes, J. & Van der Laat, R., 2000. Geophysical studies of the recent 15-year eruptive cycle at Poàs Volcano, Costa Rica, *J. Volc. Geotherm. Res.,* **97,** 425–442.

Sanderson, T.J.O., 1982. Direct gravimetric detection of magma movements at Mount Etna, *Nature,* **297,** 487–490.

Sharma, P.V., 1986. *Geophysical Methods in Geology,* Elsevier, New York.

Shaw, H.R., 1980. The fracture machanisms of magma transport from the mantle to the surface, in *Physics of Magmatic Processes,* pp. 201–264, ed. Hargraves, R.B., Princeton University Press, Princeton.

Smithsonian Institution, 1998. *Bulletin* November, **23**.

Smithsonian Institution, 1999. *Bulletin* June–September, **24**.

Torge, W., 1981. Gravity and height variatons connected with the current rifting episode in northen Iceland, *Tectonophysics,* **71,** 227–240.

Torge, W., 1989. *Gravimetry,* de Gruyter, Berlin.

Watermann, H., 1957. Über systematische Fehler bei Gravimetermessunger. DGK, München, **21**.

Wilson, L. & Head, J.W.I., 1981. Ascent and eruption of basaltic magma on the Earth and Moon, *J. geophys. Res.,* **86,** 2971–3001.

Wong, T.-F. & Walsh, J.B., 1991. Deformation-induced gravity changes in volcanic regions, *Geophys. J. Int.,* **106,** 513–520.